

# **COMFORT – Data-Driven Analysis and Simulations of Human Comfort in Office Rooms**

**Gerald FEICHTINGER<sup>1</sup>, Heimo GURSCH<sup>1</sup>, Eike SCHLAGER<sup>1</sup>, Daniel BRANDL<sup>2</sup>,  
Markus GRATZL<sup>3</sup>**

<sup>1</sup> Know-Center GmbH Research Center for Data-Driven Business and Big Data Analytics, Inffeldgasse 13/6, A-8010 Graz, Tel.: +43 316 873 30824, gfeichtinger@know-center.at, <http://www.know-center.at>

<sup>2</sup> Technische Universität Graz – Institut für Wärmetechnik, Plüddemanngasse 25/B/V, A-8010 Graz, Tel.: +43 316 873 7301, daniel.brandl@tugraz.at, <https://www.tugraz.at/institute/iwt/home/>

<sup>3</sup> Fachhochschule Salzburg – SMART BUILDING | SMART BUILDINGS IN SMART CITIES, Markt 136a, 5431 Kuchl, Tel.: +43 50 2211 2706, markus.gratzl@fh-salzburg.ac.at, <https://www.fh-salzburg.ac.at/smb/>

## **Abstract:**

The objective of project COMFORT is the analysis of perceived human comfort in offices using several modelling approaches such as data-driven analyses, building energy simulation tools and computational fluid dynamic simulations. As part of COMFORT, this work focuses on the prediction of direct irradiance using real weather data since these physical parameters are essential input parameters for the building simulations but are not available as measurement data for the investigated region of Deutschlandsberg. The direct irradiance is predicted using polynomial regression of 3<sup>rd</sup> and 4<sup>th</sup> order of different measurements such as global irradiance, cloudiness and seasonality. The models using polynomials of 3<sup>rd</sup> order produce good results whereas the models with polynomials of 4<sup>th</sup> show a tendency of overfitting. Finally, all prediction results are used in the building simulations to analyse the impact of these prediction approaches and to advance the coupling of different building simulation models. The building simulations show that the difference between the prediction results are small and negligible.

## **Keywords:**

Global/Direct/Diffuse Irradiance, Linear Regression with Polynomials, Building Energy Simulation, Computational Fluid Dynamics

## **1 Introduction**

Comfort conditions in rooms and buildings are currently poorly recorded and maintained by the building management due to a lack of appropriate sensors, data management and data analytics. New solutions are required to maintain satisfactory room conditions while achieving optimal energy efficiency. Project COMFORT combines aggregated and enriched data from sensors and simulations to quantify, evaluate and optimise the perceived human comfort in regard of temperature and air quality while taking economic considerations into account. Approaches new to building automation, including machine learning, multi-source data fusion, virtual sensors, simulations, wireless sensor systems and coupling with building information modelling are used to understand human comfort by analysing multi-modal and heterogeneous

data. Thereby, a predictive and concise representation of comfort conditions in rooms and buildings is created. This is researched and investigated in two different test spaces; the first one is a dedicated testing site consisting of two Test Boxes simulating offices in Graz; the second one is an office building in Deutschlandsberg.

A central project objective is to augment the collected sensor data so that statements about thermal comfort can be made. Influencing factors on thermal comfort of humans are parameters such as clothing, activity, air temperature (even at different room heights), surface temperatures of the surrounding environment, air humidity and flow velocity. Since not all of these influencing factors can be measured, building energy simulations (BES) and flow simulations are used to augment measured data. The greatest challenge in this regard is the air flow in the rooms of the test spaces, since it is determined by a large number of influencing variables in addition to the room geometry. Computational Fluid Dynamics (CFD) simulations are used to capture the air flow, including supply and exhaust air flow, surface temperatures, heat input by people, equipment and lighting, and solar irradiance.

A major influencing factor in all mentioned simulation models is the outdoor climate. While air temperature, humidity, air pressure, wind speed and direction can be measured comparatively easy and thus are available in good quality for a large number of locations, the situation is somewhat different for solar irradiance. Above all, it is crucial to split up the easy-to-measure global irradiance into direct and diffuse irradiance to correctly quantify additional interior heat gains caused by their varying absorption, reflection and transmission characteristics<sup>1</sup> of windows. Thus, measured global irradiance  $R_{glob}$  has to be split into its components of direct irradiance  $R_{dir}$  and diffuse irradiance  $R_{diff}$ . These components are not available as measurements but only global irradiance is measured in Deutschlandsberg. Due to the direct relationship between the components, defined as

$$R_{glob} = R_{dir} + R_{diff} ,$$

it suffices to model only one of the two components, either  $R_{dir}$  or  $R_{diff}$ . As stated in the subsequent sections, this work focuses on the data-driven prediction of the direct irradiance  $R_{dir}$ , using several impact factors such as cloudiness and season. Both components, direct and diffuse irradiance, serve as input parameters for the BES and the CFD simulations.

In literature [7], several notations for the term solar radiation in general are used. Solar radiation serves as hypernym for solar irradiance and solar irradiation, whereas solar irradiance is defined as power per square meter ( $W/m^2$ ). Solar irradiation, instead, is the integration of solar irradiance over time and is defined as energy per square meter ( $J/m^2$ ). Moreover, two measuring types of solar irradiance have to be distinguished, namely solar horizontal irradiance and solar normal irradiance. In the following, global irradiance and direct irradiance is uniformly addressed by the means of horizontal measurements whereby diffuse irradiance is isotropic and is therefore independent on the angle of incidence of the sun.

---

<sup>1</sup> The sum of absorption, reflection and transmission is always 100 percent.

The remainder of this paper addresses several questions regarding the prediction of direct and diffuse irradiance: How suitable are polynomial regression approaches to predict direct and diffuse irradiance? Are the global irradiance and the cloudiness sufficient to predict the diffuse irradiance? What is the achievable level of error? What effects do different prediction approaches have on the BES simulation and the CFD simulation? Does the standard assumption of a 20% share of diffuse irradiance that is used in CDF simulations hold in any weather situation?

## 2 Method

The entire presented model framework consists of several sub-models which are interdependent on each other. Sub-models and interdependencies are outlined in the remainder of this section.

### 2.1 Model Design

Figure 1 shows the general model design consists of two data sources and three sub-model approaches. The Polynomial Regression Modelling (PRM), which is a data-driven model using regression with polynomial functions, predicts direct and diffuse irradiance based on the input parameters global irradiance and cloudiness. Its results serve as input factors to the other two sub-models, the building simulation approaches BES and CFD, by the combination of which thermal comfort in single office rooms is analysed. For the current investigations the BES and CFD simulation tools act independently from each other. In future, deeper investigations with two ways of coupling, firstly, a unilateral (BES to CFD) and, secondly, a bilateral (BES to CFD and vice versa) model coupling, are planned. This is indicated by the dashed connecting arrows in Figure 1.

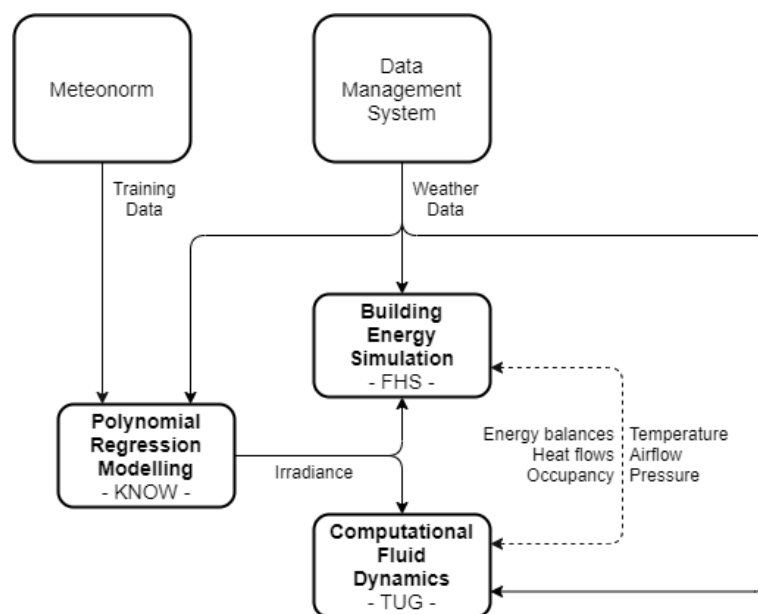


Figure 1: General modelling framework

## 2.2 Data Sources

As indicated in Figure 1, the available data sources consist of a newly developed Data Management System (DMS) and some virtual training data provided by Meteonorm [4]. All sensor data, weather data along with its corresponding meta data is collected and stored in the DMS. The DMS is accessible for all project partners via an HTTP interface for automatic querying and a web interface for human interaction. The available data sets in the DMS include:

- Building services engineering systems data derived from existing building infrastructure in the test offices, like room temperature, outdoor temperature, cooling, heating and several upper and lower limit parameters to control the system. This data set is available in a 15-minute interval starting from September 2019. [2]
- Reference measurements collected by special measuring instruments located in the test offices representing a validated ground truth, including room and surface temperatures, heat transfer, humidity, wind speed and CO<sub>2</sub> concentration. This data set is available in a 6-second interval starting from July 2019. [2]
- Measurements like temperature, cooling, heating from two Test Boxes running at controlled laboratory conditions located at Graz University of Technology. This data set is available in a 1-second interval starting from July 2019. [2]
- Live weather data for the test area Deutschlandsberg, including outdoor temperature, humidity, global irradiance, pressure, wind speed and wind direction. This data set is available in a 10-minute interval starting from September 2019. [3]
- Live weather data for the test area Deutschlandsberg, like cloudiness, humidity, pressure, temperature, wind conditions, wind direction/speed. This data set is available in a flexible change-of-value interval starting from December 2019. [5]

Finally, a virtual weather dataset of a weather model generating global, direct and diffuse irradiance, temperature, cloudiness, sunshine and rain is available with a 1-hour sampling interval for selected representative years [4], but is not stored in the DMS due to its limited use in the Comfort project.

## 2.3 Polynomial Regression Modelling

Since no measurement of direct and diffuse irradiance for the area of Deutschlandsberg exist, a data-driven prediction of these quantities is required. The prediction is based on measured data available for this region including global irradiance [3] and cloudiness [5], supplemented by the information of the season. Several quantities such as cloudiness, rainfall, snow, along with the constitution of the surrounding have an influence on the diffusion of the irradiance [8]. By using training data from the same location, the constitution of the surroundings is incorporated. Furthermore, only those variables are considered which are also measured, i.e., are available in the DMS as measurements.

The available virtual weather data for Deutschlandsberg stretches over four years, that were used for training [4]. One year of measurement data was subsequently used for testing. The hourly sampled training data includes global irradiance, direct and diffuse irradiance, cloudiness and temperature. Some additional quantities that are available in the training data such as sunshine could theoretically also be used for training and potentially also enhance the

performance of the trained model. But they cannot be used, since these quantities are not measured and hence are not part of the live weather data.

In order to predict direct irradiance, a polynomial regression was used modelling the relationship between independent variables and one dependent variable. For  $k$  independent variables  $x_1, \dots, x_k$  and the direct irradiance  $R_{dir}$  being the dependent variable, the approach for a polynomial regression of degree  $n$  is

$$R_{dir} = \sum_{i_1=0}^n \sum_{i_2=0}^{n-1} \dots \sum_{i_k=0}^{n-i_{k-1}} \alpha_{i_1, \dots, i_k} \prod_{i=1}^k x_i^{i_k}.$$

The coefficients  $\alpha_{i_1, \dots, i_k}$  are computed by minimizing the residual sum of squares between the measured direct irradiance and the direct irradiance predicted by the polynomial regression. To measure the quality of regression using polynomials of different order, or including different features, the coefficient of determination ( $R^2$ ), the mean error<sup>2</sup> ( $ME$ ), the root mean squared error and the maximum absolute error were used.

Besides the use of different features and different polynomial orders, the seasonal effects are considered. To do this, a year was split into four seasons, each season centred around the equinoxes and solstices, respectively. The information about the season was handled in three different ways. A first and simple approach trains on training data of the whole year at once; a second approach includes information which season it is as an additional feature; a third approach trains on every season separately, therefore computing coefficients suitable for this specific time interval only. The third approach has the advantage that the results for different seasons can be compared, thus revealing if the prediction quality varies with respect to the seasons.

## 2.4 Building Energy Simulation

A comprehensive BES approach was developed to predict expected thermal comfort in a zone, like a single room or more rooms that are considered to be a common zone. In this work, a typical office room is used to evaluate the effects of the different prediction approaches for solar irradiance presented above. This office room is located on the 2<sup>nd</sup> floor in the office building in Deutschlandsberg and has a maximum capacity of eight people and is south facing. The building and plant model<sup>3</sup> are based on the "as-built" documents provided by the building user, including the building physics information about component structures and characteristic values of windows and glazing. Its main input variables consist of climate data like air temperature, outside air humidity, wind speed, wind direction and global irradiance, whereas the latter was split into direct and diffuse irradiance using the PRM. Based on the PRM results, the direct horizontal radiation is converted into direct radiation that is normal to the window using a set of climate data consisting temperature, humidity, wind direction and wind speed.

---

<sup>2</sup> Mean over the difference between prediction and measurement.

<sup>3</sup> Software: IDA ICE (Equa, Version 4.8, SP1)

Solar shading on the object has a considerable effect on the simulation results. For that reason, all approaches given were considered for two scenarios. Firstly, the sun protection from external venetian blinds was assumed to be deactivated. Secondly, the sun protection was controlled depending on the direct irradiance with an activation of the sun protection at  $100 \text{ W/m}^2$ . Furthermore, the simulation ran through the specified investigation period 14 times in order to achieve a steady state of the building and system technology and thus to provide stable results.

In order to highlight the impact of the direct irradiance, minor adaptations in the simulation model were made. The most important adaptation concerns the heating and cooling of the examined room. In order to be able to use the operative temperature as a meaningful result variable, heating and cooling were deactivated and the supply air was introduced almost adiabatically with a temperature of  $21 \text{ }^\circ\text{C}$ .

## 2.5 Computational Fluid Dynamics

To complement the BES, a CFD simulation approach<sup>4</sup> was developed to simulate thermal office operations. The main goal of CFD simulations is to provide very detailed observations of the thermal behaviour targeted at the identification of local discomfort such as hot and cold spots or too high air velocities. Firstly, CFD simulations were created and calibrated using the two Test Boxes located at the campus Inffeldgasse at Graz University of Technology. By using these Test Boxes, the thermal behaviour was monitored under controlled conditions allowing a comprehensive validation of the simulations results. Secondly, these simulation approaches were used to simulate the same office room as for the BES located in the office building in Deutschlandsberg.

The CFD model of the office room's interior air space was selected to compare the heating effects caused by direct irradiance predicted by the PRM presented in Section 2.3. Since the CFD model uses a solar simulator model, the measured horizontal (global) irradiance has to be converted into the beam direction which is changing during the day. As boundary condition the value of the direct irradiance and three direction vectors are required which can be extracted in terms of the solar altitude and the azimuth angle from the solar position diagram. The solar simulator already contains the solar position diagrams, therefore only the geographic position and the date is required as input for simulation. Before conversion, the irradiance is split into direct and diffuse fraction using the PRM approach. The diffuse irradiance is not converted into the direction of irradiance, since it is assumed that it is approximately evenly distributed from different directions. A window absorbs almost the entire diffuse irradiance whereby this quantity is neglected in the simulation.

Furthermore, the model contains the interior air space, all equipment, furniture and the occupants whereas the thermal mass is not considered. Therefore, heat fluxes are set at the corresponding surface boundaries to capture the influence of the internal thermal gains caused by equipment such as notebooks, monitor or lighting. Similarly, a heat flux was defined representing the activity of the occupants but not considering transpiration effects and  $\text{CO}_2$  production although this consideration would be an option.

---

<sup>4</sup> Software: Fluent (ANSYS)

### 3 Results

The results are split into three main sections in accordance with the general modelling framework. Section 3.1 illustrates the PRM to split the solar irradiance into its direct and diffuse parts were investigated by using four different prediction approaches. Two scenarios for BES are demonstrated in Section 3.2, each of them covering the predictions of the four PRM approaches as input parameters. The CFD simulations in Section 3.3 present the results of five scenarios, where all four PRM prediction approaches are supplemented by a scenario assuming a 20 % share of diffuse irradiance. While the prediction of the irradiance was done for the period from the 18<sup>th</sup> to the 31<sup>st</sup> of December 2019, the comparison with the BES and the CFD results are illustrated for the 18<sup>th</sup> of December 2019 only, due to the considerable computational effort of the CFD simulation.

#### 3.1 Polynomial Regression Modelling

The regression model should be capable of splitting the global irradiance into its components direct and diffuse irradiance by employing cloudiness (*CLOU*) and the season as additional model input. Figure 2 depicts the relationship between global and direct irradiance of the measured data (blue dots) and the predicted data (red line) using global irradiance, cloudiness and the seasons as features. In Figure 2a, the simplest approach is considered, namely using polynomials of order one, resulting in predictions with significant deviations from the real values. Regressions using polynomials of order two (Figure 2b), three (Figure 2c) and four (Figure 2d) all catch the nonlinear relationship between the global and the direct irradiance quite well. Looking at the mean error, one can observe that the prediction tends to overestimate the actual data. The predicted values are aligned along nine rays due to the classification of the cloudiness in nine different levels (octas) between zero and one. Thus, each ray corresponds to a cloudiness level.

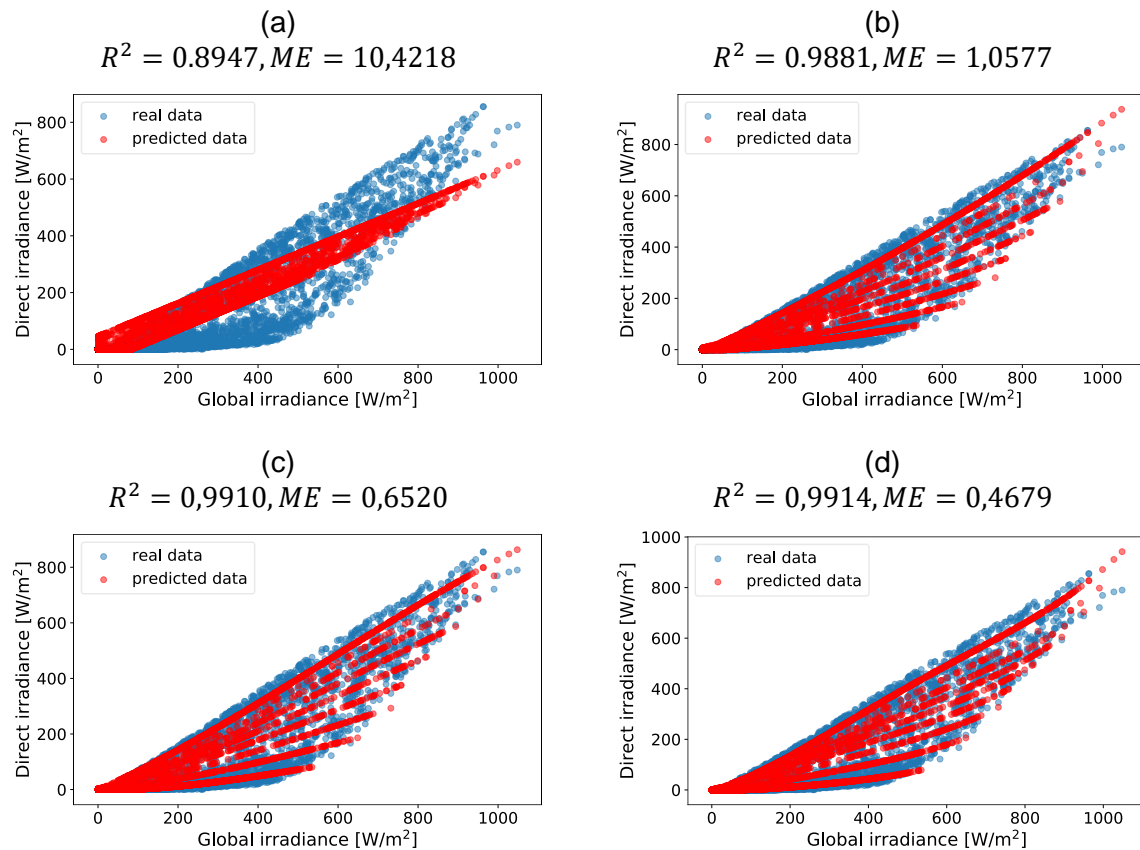


Figure 2: Relationship between direct irradiance and global irradiance with respect to the cloudiness level for models with polynomials of order (a) one, (b) two, (c) three and (d) four.

An illustration of the regression coefficients undermines the potential seasonal variation within a year. Figure 3a compares the results for five models considering global irradiance and cloudiness as features. The first model is trained on data of a whole year<sup>5</sup> (black circles) and the other four are trained on the four seasons<sup>6</sup> centred around the winter solstice (blue stars), equinox in spring (orange stars), summer solstice (green stars) and equinox in fall (red stars). The coefficients for the season around the equinox in spring and the equinox in fall are very similar, as the sun altitude is the same at the equinoxes, whereas the coefficients for the time around the winter solstice are smaller and higher for the summer solstice. Figure 3b lists the model coefficients and their physical meaning in all of the five models.

---

<sup>5</sup> Yearly coefficients cover always the whole year, i.e., twelve months.

<sup>6</sup> Seasonal coefficients cover in total three months around the respective cut-off day.



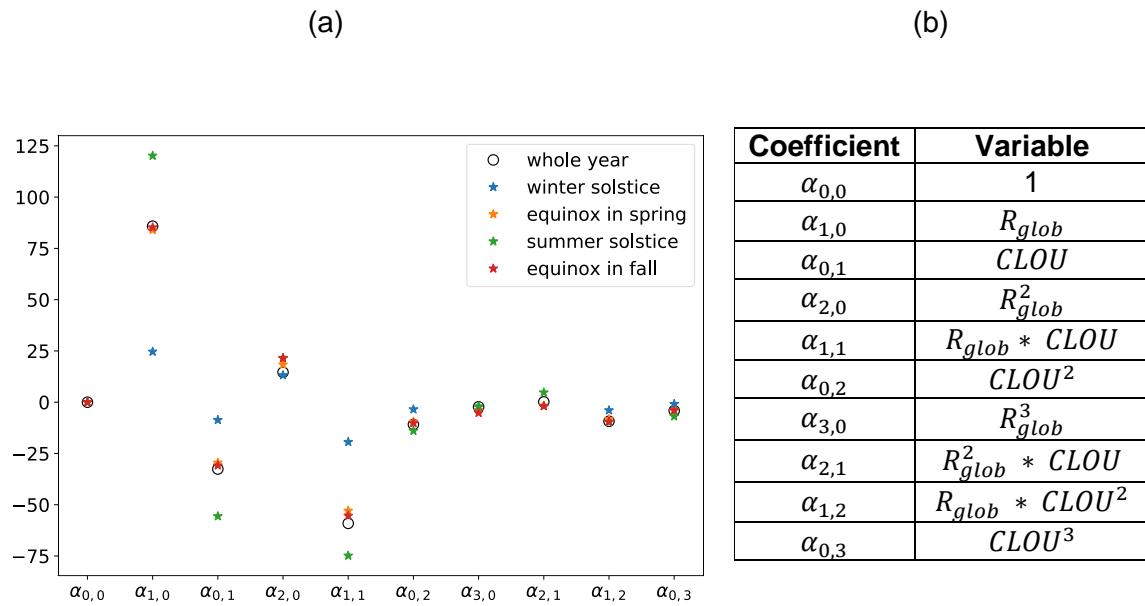
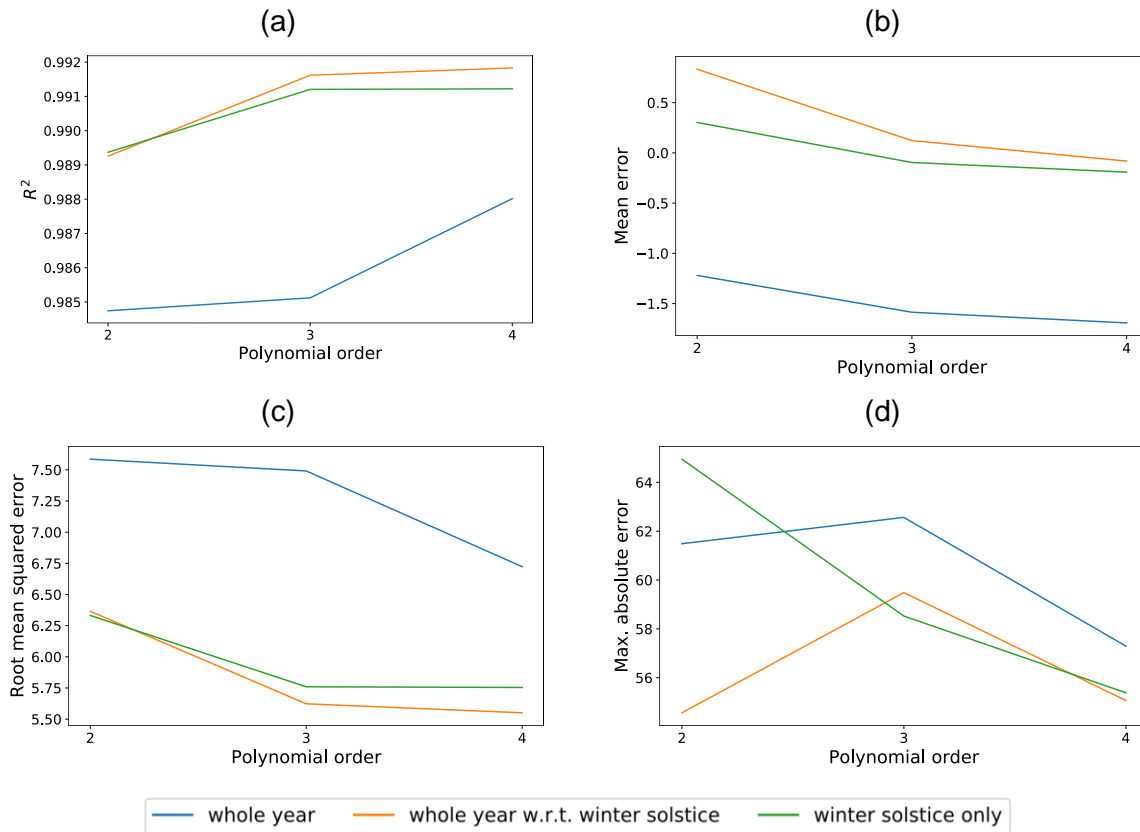


Figure 3: (a) Comparison of the regression coefficients for models trained on the whole year and on every season separately; (b) table of model coefficients and their physical meaning.

In order to examine the influence of the seasonality in more detail, a model trained on yearly data excluding information of the season, a model also fitted on the whole year but including information of the season, as well as a model fitted on the season around winter solstice only, were compared. All three approaches were conducted with polynomials of order two, three and four, and tested on data around winter solstice only. Figure 4 illustrates the polynomial order of the models and their achieved error rates, where Figure 4a shows coefficients of determination  $R^2$ , Figure 4b depicts the mean error, Figure 4c shows the root mean squared error and Figure 4d shows the maximum absolute error. The approaches that take seasonal effects and polynomials of order three and four into account tend to fit better due to a higher coefficient of determination and a lower absolute value of mean error, root mean squared error and maximum absolute error whereas the model trained on yearly coefficients excluding seasonal information lacks of accuracy. Moreover, the model approach trained with 4<sup>th</sup> degree polynomials may tend to overfitting. The latter may be confirmed by comparing the errors of the polynomials all four seasons as illustrated in Figure 13 in the appendix.



**Figure 4:** Error measurements for the model approaches for a yearly trained model excluding seasonal information (blue), one including seasonal information (yellow) and one trained on data around winter solstice only (green) are compared:: (a) coefficients of determination, (b) mean error, (c) root mean squared error, (d) maximum absolute error.

Based on the results so far, four different models were selected to predict the direct irradiance and evaluate the results further with the BES and CFD simulation, namely,

- I. a model using 3<sup>rd</sup> polynomials and training on the whole year including the season as a feature ( $R_{dir}^{y,3}$ ),
- II. a model using 3<sup>rd</sup> order polynomials and training on winter data only ( $R_{dir}^{s,3}$ ),
- III. a model using 4<sup>th</sup> polynomials and training on the whole year including the season as a feature ( $R_{dir}^{y,4}$ ) and
- IV. a model using 4<sup>th</sup> polynomials and training on winter data only ( $R_{dir}^{s,4}$ ).

The global irradiance and cloudiness measurement data supplemented by the predicted values for direct irradiance in the evaluation period from the 18<sup>th</sup> to the 31<sup>st</sup> of December 2019 are illustrated in Figure 5. On two days (21<sup>st</sup> and 22<sup>nd</sup>) the global irradiance is really low with approximately 50 W/m<sup>2</sup>, on three other days (19<sup>th</sup>, 23<sup>rd</sup> and 27<sup>th</sup>) global irradiance is moderately high in the area of 200 W/m<sup>2</sup>, whereas on all other days it reaches up to 350 W/m<sup>2</sup>. A contrary relation between cloudiness and global irradiance is implied.

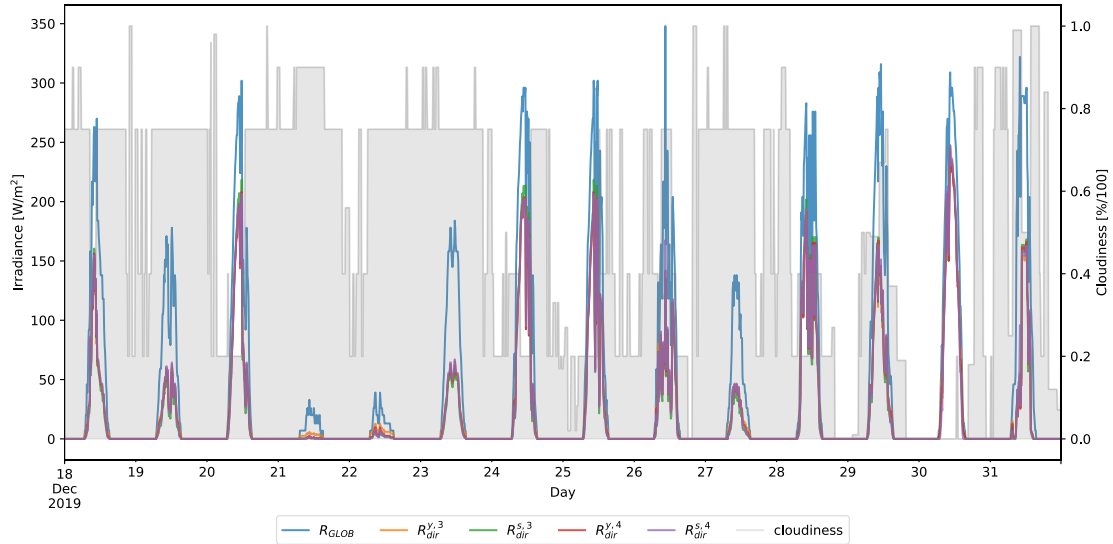


Figure 5: Results for different models supplemented by real measurement data for global irradiance and cloudiness from the 18<sup>th</sup> until the 31<sup>st</sup> of December 2019.

Figure 6a focuses on selected predictions of direct irradiance from global irradiance ( $R_{glob}$ ) and the cloudiness level ( $CLOU$ ) of the 18<sup>th</sup> of December 2019. The differences between the prediction approaches are small. This insight is confirmed by Figure 6b, which shows differences in the direct irradiance of about  $\pm 7.5$  W/m<sup>2</sup> between the approaches and the baseline regression using 3<sup>rd</sup> order polynomials and training on the whole year<sup>7</sup>.

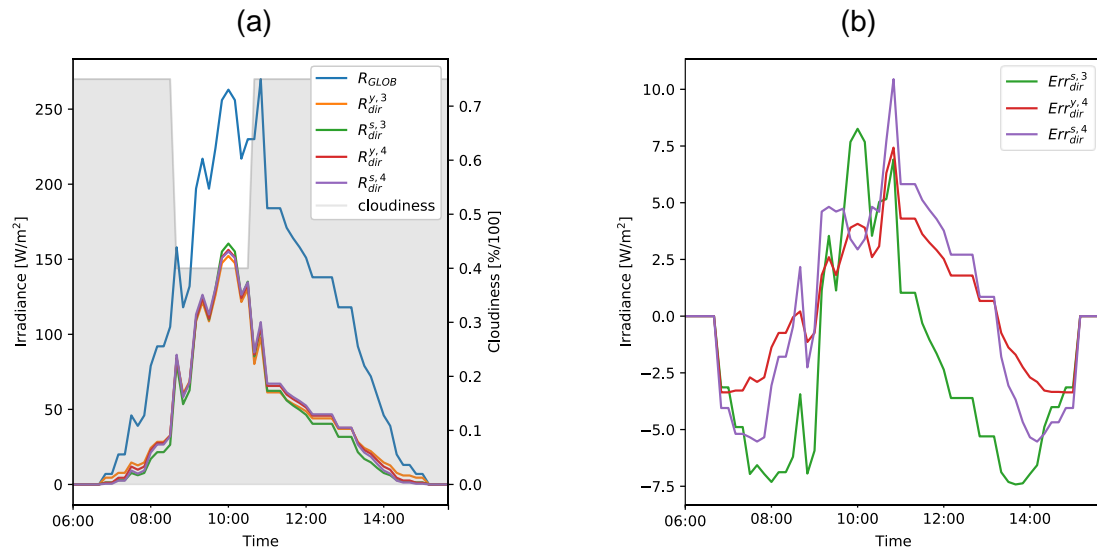


Figure 6: (a) global irradiance, cloudiness level and predicted direct irradiance for four different prediction approaches for 18<sup>th</sup> of December 2019; (b) absolute differences between the prediction approaches for 18<sup>th</sup> of December 2019.

<sup>7</sup> Defined as:  $Err_{dir}^{s,3} = R_{dir}^{s,3} - R_{dir}^{y,3}$ ,  $Err_{dir}^{y,4} = R_{dir}^{y,4} - R_{dir}^{y,3}$ ,  $Err_{dir}^{s,4} = R_{dir}^{s,4} - R_{dir}^{y,3}$

### 3.2 Building Energy Simulation

In this section, the influence of the prediction difference between the four selected models on BES are investigated deeper. The yearly approach with 3<sup>rd</sup> order polynomials  $R_{dir}^{y,3}$  is selected as baseline for these investigations. All results are depicted as the difference between the results of the other three models and the base line  $R_{dir}^{y,3}$ . These differences are figured as absolute differences with respect to the quantity that is observed such as solar gains or temperature. The simulation took place in time steps with a length of 30 minutes that have been aligned to hourly steps for the purpose of uniformity across all modelling approaches. To demonstrate the effects of solar irradiance on the comfort in the office room the operative temperature in the centre of the room, natural lighting of the workplace at the window workplace, activation of the sun protection and solar entries through a window were selected. These results are illustrated in Figure 7 comparing two scenarios: one without a sun protection (NO\_SHADE), and one scenario that assumes a sun protection (SHADE) over the windows<sup>8</sup> on 18<sup>th</sup> of December 2019.

For the scenario NO\_SHADE, the solar gains through a window in the office without sun protection is depicted in Figure 7a, Figure 7c and Figure 7e. The solar gains through windows highly correlate with the prediction results for the direct irradiance. The differences between the prediction approaches are neglectable. The resulting differences in the operative temperature in the office highly correlate with the solar gains showing a sharp increase before midday as shown in Figure 7c. Again, the differences between the prediction approaches are negligible. Finally, Figure 7e shows the illumination for a workstation at the window is for all four prediction approaches similar to solar gains throughout the day with a small absolute error.

In the scenario SHADE an automated irradiance-based regulation of a sun protection, i.e. shades, on the windows was considered and the results are shown in Figure 7b, Figure 7d and Figure 7f. As seen in Figure 7b, the activation of the sun protection<sup>9</sup> starts around 10 am in the morning after the global irradiance crosses a certain activation level. There is almost no difference in the activation behaviour between the prediction approaches with the except for the seasonal approach with 3<sup>rd</sup> order polynomials  $R_{dir}^{s,3}$ , in which the sun protection was activated one simulation step of 30 minutes earlier. In Figure 7d the effect of the sun protection on the operative temperature is reflected, whereas the variation between the prediction approaches is again negligible. Compared to the NO\_SHADE scenario, the absolute level of operative temperature is about 1.5 °C lower throughout the day. A similar effect may be obvious in the development of the illuminance as shown in Figure 7f. A slight delay due to the activation of the sun protection and again small differences between the prediction approaches of about ±20 lux is to be mentioned here. When looking at the seasonal approach with 3<sup>rd</sup> order polynomials  $R_{dir}^{s,3}$ , the effect of the earlier activation of the sun protection can be seen as well.

---

<sup>8</sup> In the test offices manual shades are mounted on the windows, whereas in the simulation a fully automated shading tool is assumed. A more realistic approach is currently being developed.

<sup>9</sup> A full activation of the sun protection is represented by one whereas zero is equivalent to a fully deactivated sun protection.

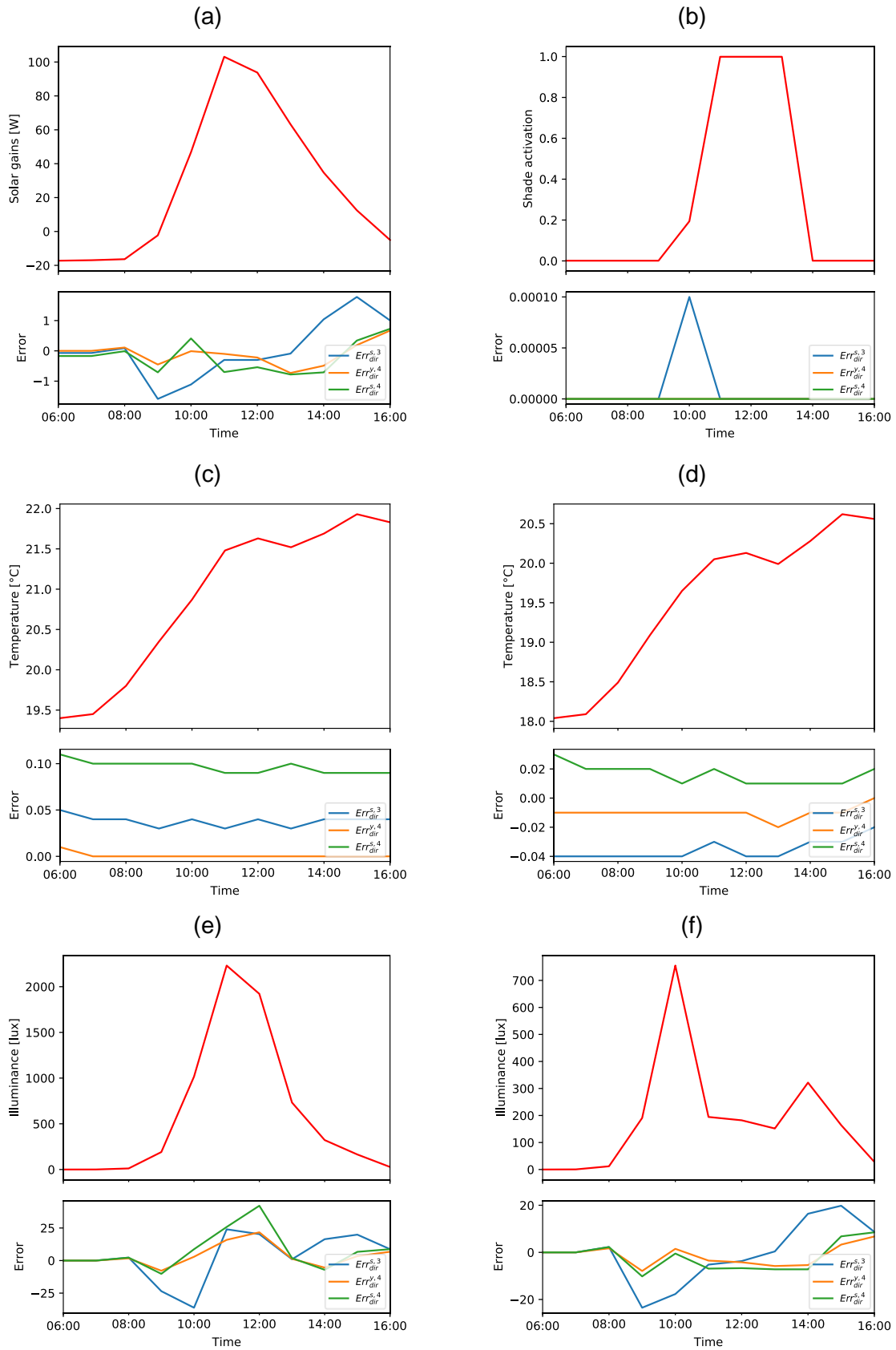


Figure 7: BES results for the 18<sup>th</sup> of December 2019 for two scenarios: (a) Solar gains (NO\_SHADE), (b) Shade activation (SHADE), (c) Operative temperature (NO\_SHADE), (d) Operative temperature (SHADE), (e) Illuminance (NO\_SHADE), (f) Illuminance (SHADE)

### 3.3 Computational Fluid Dynamics

For the comparisons, a period over eight hours with hourly<sup>10</sup> changing climate was simulated: from 8 am to 4 pm in time steps with a length of one hour each. It is assumed to keep the internal heat loads and the heat transfer between neighbouring rooms constant. No shading device was considered in the CFD model. The measured climate data from 18<sup>th</sup> of December 2019 were used as boundary condition in the simulations, the diagrams in Figure 8 are illustrating sun duration and sun position at this day. A virtual layer was defined on the exterior wall of the office room representing the thermal resistance to the exterior environment at varying exterior air temperature. The solar irradiance intensity is used as varying boundary condition over the entire simulation period.

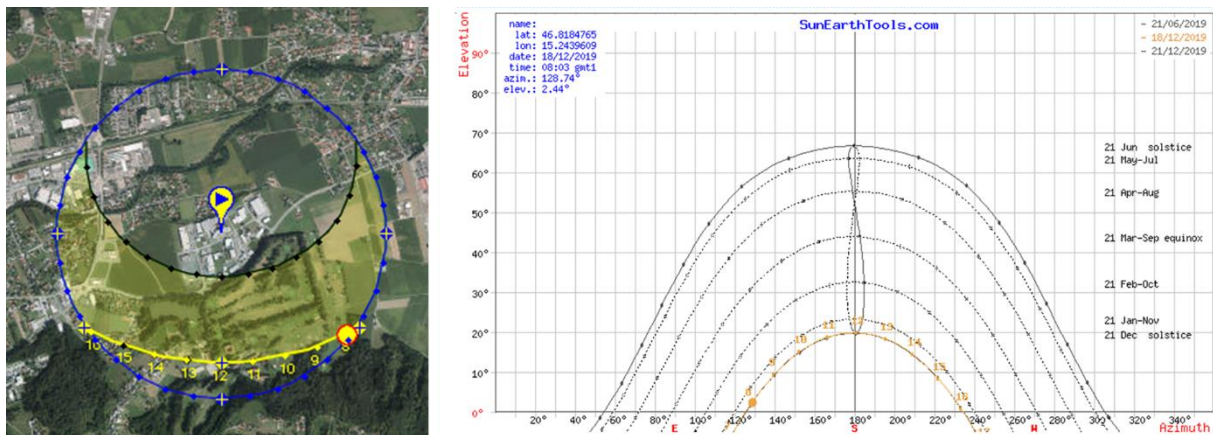


Figure 8: Illustration of sunshine duration and sun position for December 18<sup>th</sup> 2019 [6]

Figure 9 shows the initial CFD model steady state start calibration based on temperature contours for the simulated office room on the 18<sup>th</sup> of December 2019 at 8 am in the morning. Obviously, several factors like windows, screens, and lightning which cause varying temperature levels have an impact on the CFD simulations.

The simulation results consider five different modelling approaches for direct and diffuse irradiance. Like in the case of BES, the yearly approach with 3<sup>rd</sup> order polynomials  $R_{dir}^{y,3}$  for predicting the direct irradiance is selected as the baseline. The three remaining prediction approaches supplemented by a scenario with an assumption of a 20 % share of diffuse irradiance are illustrated as differences to the base scenario  $R_{dir}^{y,3}$ . The scenario with a 20 % share of diffuse irradiance ( $R_{dir}^{20\%}$ ) is a standard assumption that is only valid in cloudless weather conditions, but is commonly used in CFD simulations that may be examined and its validity evaluated.

<sup>10</sup> A further reduction to ten minutes intervals to increase the quality of the results is considered.

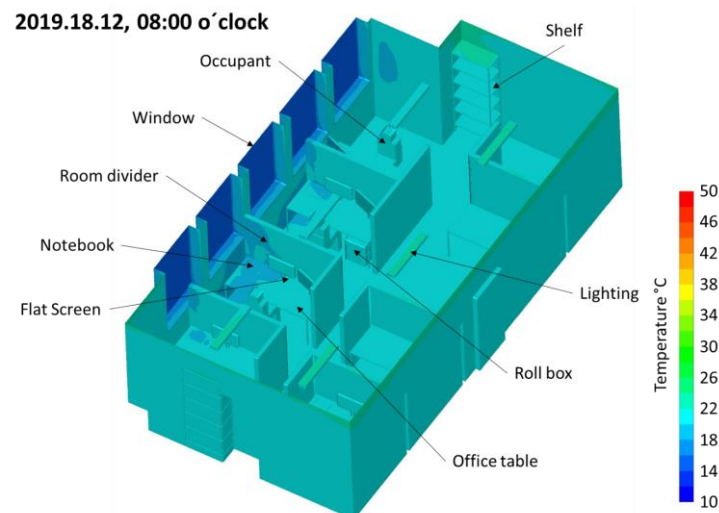


Figure 9: Initial CFD model based on temperature contours on the 18<sup>th</sup> of December 2019

In Figure 10 four main results are illustrated. The average temperature in Figure 10a shows a clear peak of around 33 °C around midday with small deviation between the remaining prediction approaches but significantly higher average temperatures for the  $R_{dir}^{20\%}$  scenario caused by the higher share of direct irradiance this model assumes. Looking at the temperatures in the office room, the heating effect of direct irradiance is confirmed showing a local peak of more than 60 °C around midday for the base scenario as depicted in Figure 10b. By contrast, average relative humidity as shown in Figure 10c has its minimum around midday again corresponding to the course in the other scenarios. In addition, the development of the average solar heat flux depicted in Figure 10d is similar to that of temperature.

These results confirm that the differences between the four data-driven prediction approaches for direct irradiance turn out to be very small, whereas a clear difference to the  $R_{dir}^{20\%}$  scenario arises. The latter may be due to too optimistic weather assumptions. Finally, the results are supplemented by Figure 11 and Figure 12 in the appendix showing the hourly sampled development of the local surface temperatures in the office for all simulations.

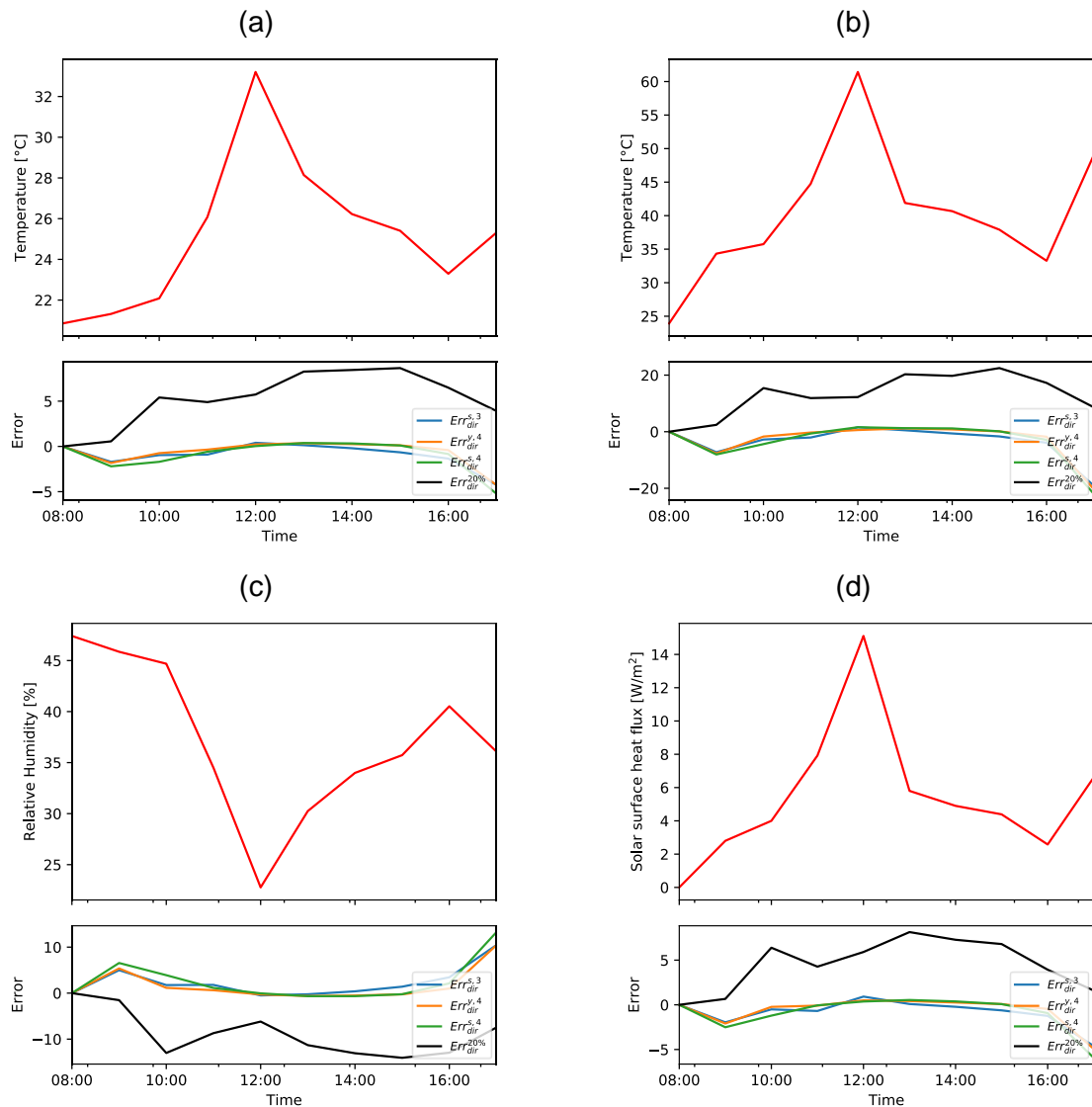


Figure 10: CFD results for the 18th of December 2019: (a) Average temperature, (b) maximum temperature, (c) average relative humidity, (d) average surface heat flux

## 4 Discussion

This work investigates the potential of regression-based prediction of direct irradiance from global irradiance and cloudiness. It was shown that the prediction approaches using polynomials of 3<sup>rd</sup> order produce good results although some predictors lack on interpretability. In order to develop a more realistic and comprehensible approach, a further deepening in this area is necessary and is considered as a next step. The difference in model and results between training on the whole year at once and training on the single seasons deserves a closer look, especially with focus on overfitting. Other features including extra-terrestrial irradiance, sun shine or relative humidity may be considered to increase the model validity and model accuracy. In addition, a closer investigation of the theory behind weather modelling and forecasting may be of interest in order to take other currently unconsidered interrelations into account. Furthermore, a comprehensive investigation of the residuals is planned.



For BES, this investigation confirms the obvious assumption that different prediction models for splitting global irradiance into direct and diffuse irradiance naturally have an influence on the results of a building simulation. The simulation results presented for a south-facing office at the Deutschlandsberg site show that the solar shading on the building has a significant impact on the effect of the different irradiance values. While short-term differences accumulate without sun protection, higher short-term differences occur with sun protection when the sun protection is activated at a different time, but these are balanced out over time. In order to be able to make a statement about the absolute quality of the different variants, a comparison of the simulation results with measured values in the examined object during the examination period would be necessary. Although these were recorded within the framework of the COMFORT project, the result values are significantly influenced by a large number of other variables. These include the real use of the room and its conditioning in relation to the operative temperature and the actual activation and deactivation of the sun protection that is manually controlled by office users to compromise between the solar gain and natural lighting.

From a CFD perspective it may be concluded, that the prediction of direct solar irradiance has a significant influence on the results compared to the conventional assumptions and estimates. In future, a more comprehensive and deeper model coupling approach between BES and CFD is desired due to two main reasons. Firstly, the general data flow for the input could be merged to reduce the sources of errors by ensuring uniform assumptions in the models such as the consideration of an identical shading mechanism. Secondly, and more importantly, an iterative exchange of essential input parameters including weather data, irradiance, shading of windows in terms of a coupling between these models would avoid unnecessary discrepancies in the main outcome parameters like the shown operative temperature in the office room in this work.

## References

- [1] Comfort Orientated and Management Focused Operation of Room condITions (COMFORT), <http://comfort.know-center.at>
- [2] COMFORT – Data Management System, Sustainable Built Environment Conference 2019, Poster
- [3] Zentralanstalt für Meteorologie und Geodynamik (ZAMG), <https://www.zamg.ac.at/>
- [4] Meteonorm – Einstrahlungsdaten für jeden Ort des Planeten, <https://meteonorm.com/>
- [5] OpenWeatherMaps, <https://openweathermap.org/>
- [6] SunEarthTools, <https://www.sunearthtools.com>
- [7] N.A. Engerer. Minute resolution estimates of the diffuse fraction of global irradiance for southeastern Australia. Solar Energy (116). 2015, pp 215-237. <https://doi.org/10.1016/j.solener.2015.04.012>.
- [8] C. Furlan, A. Pereira de Oliveira, et al. The role of clouds in improving the regression model for hourly values of diffuse solar radiation. Applied Energy (92). 2012. pp. 240-254. <https://doi.org/10.1016/j.apenergy.2011.10.032>.

## Acknowledgements

This work is part of the project “COMFORT - Comfort Orientated and Management Focused Operation of Room condITions” (No. 867533) is funded by the program ‘ICT of the Future’ (6th Call 2017) of the Austrian Research Promotion Agency (FFG) and the Austrian Ministry for Transport, Innovation and Technology (BMVIT).

The Know-Center is funded within the Austrian COMET Program—Competence Centers for Excellent Technologies—under the auspices of the Austrian Federal Ministry of Transport, Innovation and Technology, the Austrian Federal Ministry of Economy, Family and Youth and by the State of Styria. COMET is managed by the Austrian Research Promotion Agency FFG.

## Appendix

### A.1: Surface Temperatures

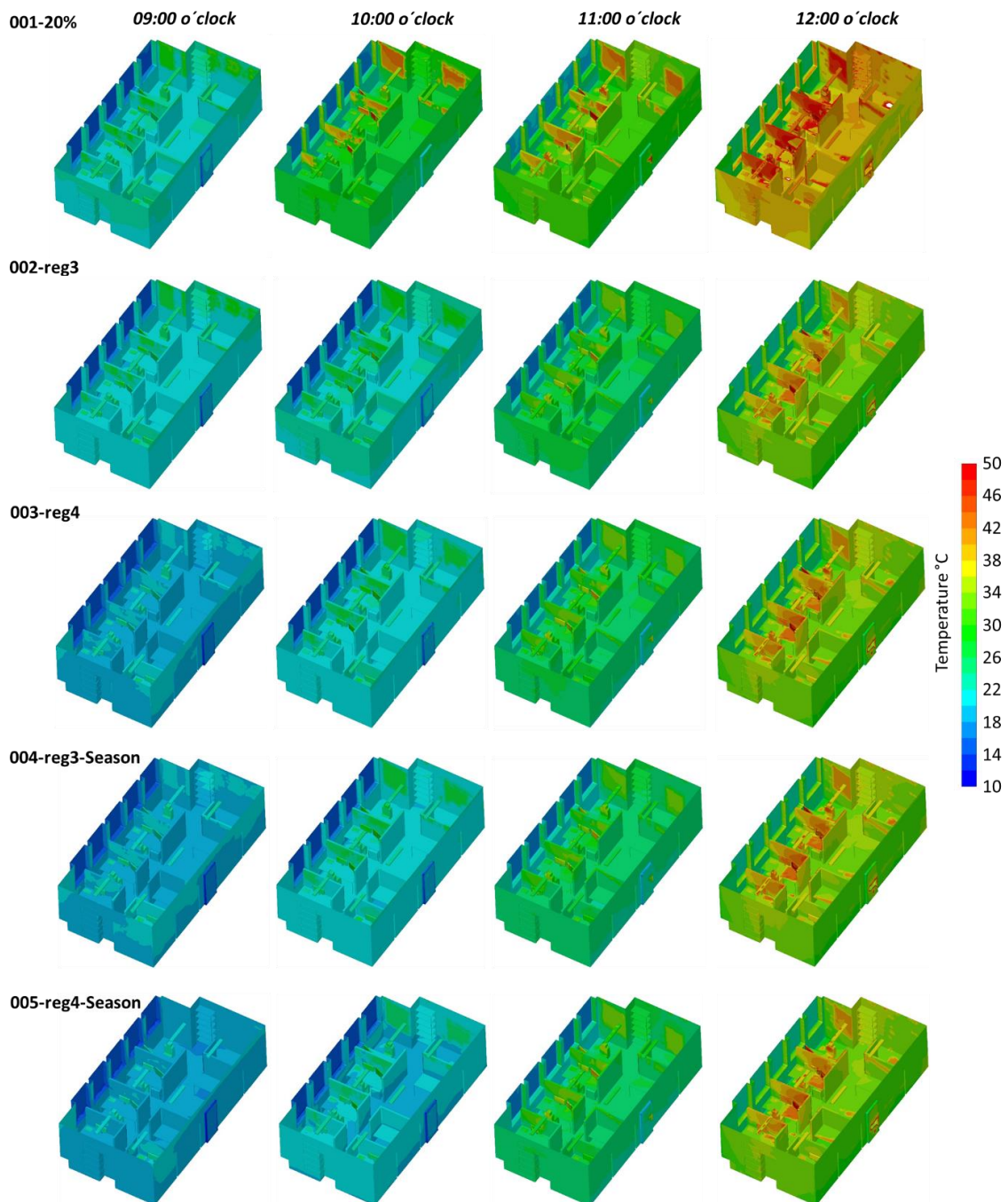


Figure 11: Comparison of surface temperature contours between the five scenarios 001 ( $R_{dir}^{20\%}$ ), 002 ( $R_{dir}^{y,3}$ ), 003 ( $R_{dir}^{y,4}$ ), 004 ( $R_{dir}^{s,3}$ ), 005 ( $R_{dir}^{s,4}$ ) in the office room from 9 am to 12 am.

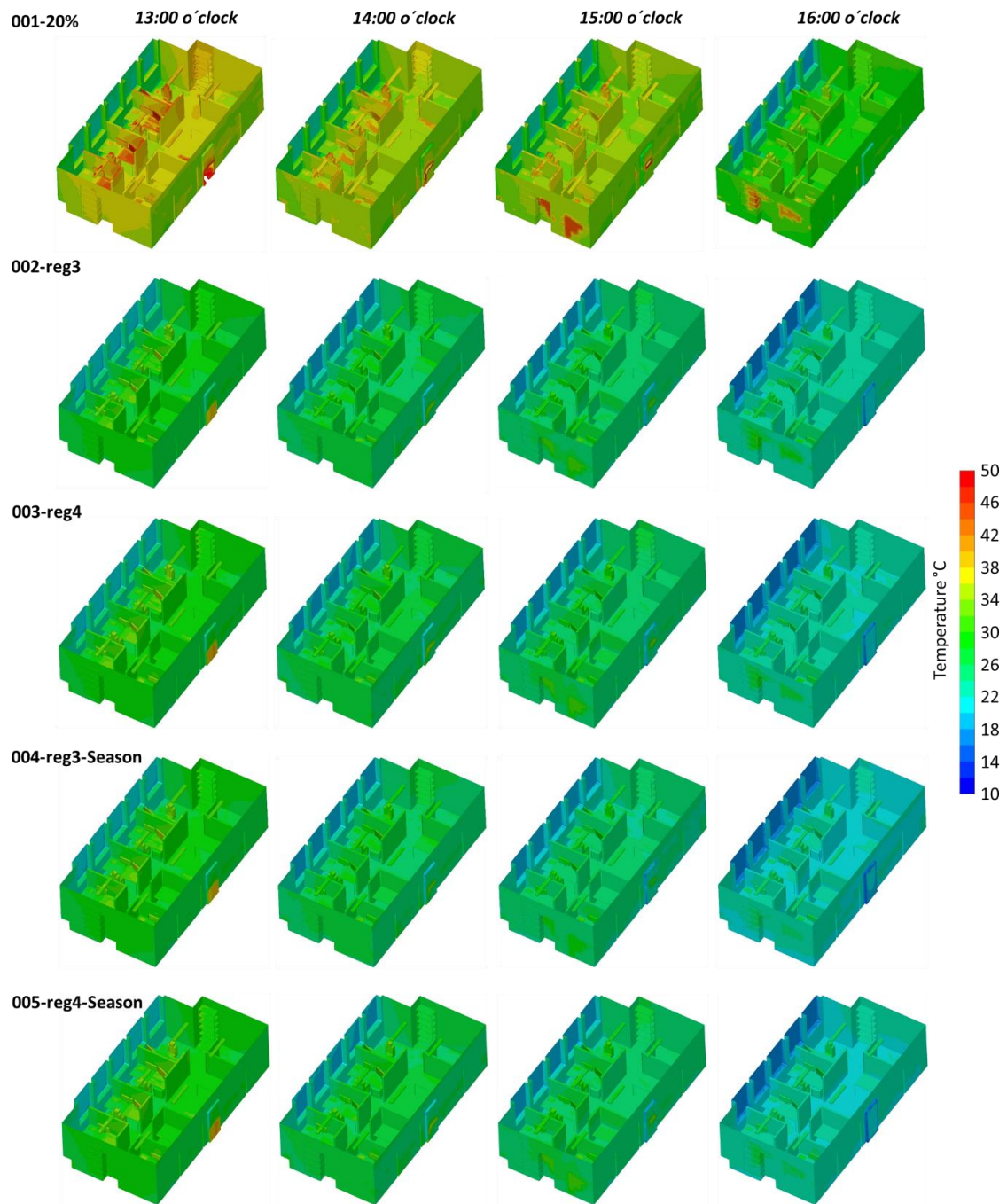


Figure 12: Comparison of surface temperature contours between the five scenarios 001 ( $R_{dir}^{20\%}$ ), 002 ( $R_{dir}^{y,3}$ ), 003 ( $R_{dir}^{y,4}$ ), 004 ( $R_{dir}^{s,3}$ ), 005 ( $R_{dir}^{s,4}$ ) in the office room from 1 pm to 4 pm.

## A.2: Error Measurements for the Polynomial Regression Modelling with Respect to the Seasons

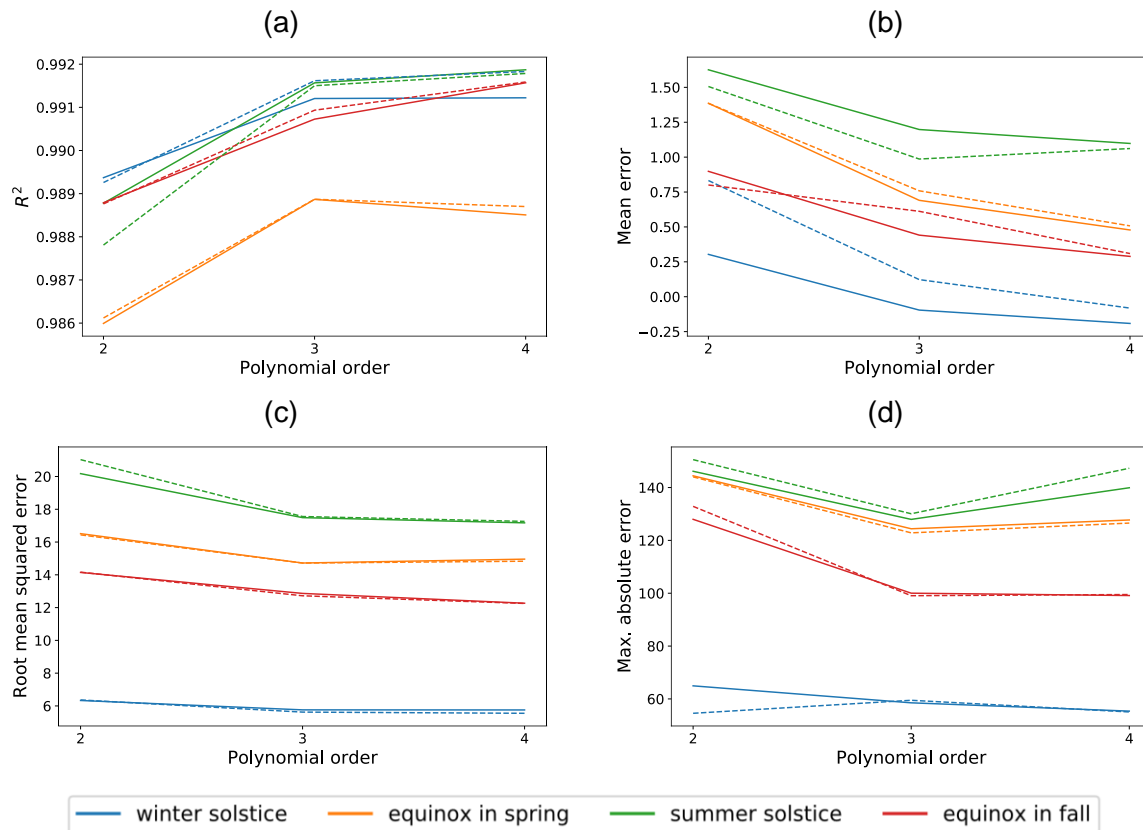


Figure 13: Error measurements for the model approaches for a yearly trained model compared to models that consider seasonal effects for all seasons: (a) coefficients of determination, (b) mean error, (c) root mean squared error, (d) maximum absolute error

The continuous lines represent the errors when trained and tested on the particular season; the dotted lines represent the errors when trained on the whole year, the season included as features and tested on data of that particular season. The performance depends on which season you look at and which error measurement you consider. I.e., either training on the whole year or with training on only the particular season is better. Looking at the mean error for time around summer solstice, training on data from spring only yields a higher value regardless of the polynomial order. At the same time, the max. absolute error is lower when training on data from spring only, compared to training on the whole year and using the seasonal information as a feature only.

Furthermore, some performance measures do not get better, or even get worse, with increased polynomial order. The  $R^2$  and the root mean squared error for the time around summer solstice only improve slightly from polynomial order of 3 to polynomial order of 4. However, the mean error and the maximum absolute error for the yearly trained data increase when using polynomials of order 4. This may indicate overfitting when using polynomials of order 4, where the sensitivity to overfitting depends on the season.